Bioconjugate Chemistry

Article

pubs.acs.org/bc

Human Transport Protein Carrier for Controlled Photoactivation of Antitumor Prodrug and Real-Time Intracellular Tumor Imaging

Xi Li,[†,‡] Jing Mu,[†,‡] Fang Liu,[†] Eddy Wei Ping Tan,[†] Bahareh Khezri,[†] Richard D. Webster,[†] Edwin Kok Lee Yeow,*[,†] and Bengang Xing*[,†]

[†]Division of Chemistry & Biological Chemistry, School of Physical & Mathematical Sciences, Nanyang Technological University, Singapore 637371

Supporting Information

ABSTRACT: Current anticancer chemotherapy often suffers from poor tumor selectivity and serious drug resistance. Proper vectors for targeted delivery and controlled drug release play crucial roles in improving the therapeutic selectivity to tumor areas and also overcoming the resistance of cancer cells. In this work, we developed a novel human serum albumin (HSA) protein-based nanocarrier system, which combines the photoactivatable Pt(IV) antitumor prodrug for realizing the controlled release and fluorescent light-up probe for evaluations of drug action and efficacy. The constructed Pt(IV)-probe@HSA platform can be locally activated by light irradiation to release the active Pt species, which results in enhanced cell death at both drug-sensitive A2780 and cisplatin-resistant A2780cis cell lines when compared to the free prodrug molecules. Simultaneously, the cytotoxicity caused by light controlled drug release would further lead to the cellular apoptosis and trigger the activation of caspases 3, one crucial protease enzyme in apoptotic process, which could cleave the recognition peptide moiety (DEVD) with a flanking fluorescent resonance energy transfer (FRET) pair containing near-infrared (NIR) fluorophore Cy5 and quencher Qsy21 on the HSA nanocarrier surface. The turn-on fluorescence in response to caspase-3 could be assessed by fluorescence microscopy and flow cytometry analysis. Our results supported the hypothesis that such a unique design may present a successful platform for multiple roles: (i) a biocompatible protein-based nanocarrier for drug delivery, (ii) the controlled drug release with strengthened therapeutic effects, (iii) real-time monitoring of antitumor drug efficacy at the earlier stage.

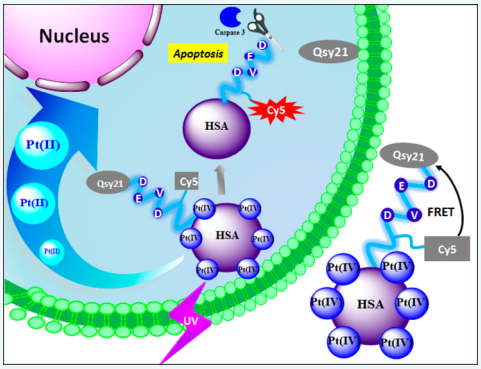

Cancer remains one of the leading causes of mortality and morbidity around the world and continues to increase with around 10 million new cases every year.[1] Although traditional cancer chemotherapy is quite benefitial in improving survial rates, it has also shown a lot of adverse effects including limited efficiency and unexpected drug resistance.[2] Directing drug molecules to cell interiors by nanocarriers is thus a promising strategy to achieve the safe and effective drug release through the enhanced permeability and retention (EPR) effect.[3−5] Among the nanoparticle-based chemotherapeutic agents, a new strategy called image-guided therapy combining the drug delivery with targeted diagnostic imaging will expand the concept of personalized therapy with improved efficiency, which therefore indicates great potential for clinical practice in the future.[6−9] Over various types of nanostructures, biocompatible protein nanocarriers, especially human serum albumin (HSA), the most abundant endogenous transport protein in human blood, could serve as an ideal platform for effective delivery of therapeutic reagents, mostly attributed to their unique features of low toxicity, minimized inflammatory stimulation, and biodegradable properties.[10,11] Up to now, the applications of HSA carrier have been successfully exploited in delivery of antitumor drug molecules, bioactive metal complexes, and multimodality imaging probes.[12−15]

So far, platinum(II)-based agents have been successfully used as powerful chemotherapeutic agents in cancer treatment due to their effective interactions with DNA nucleobases.[16−18] However, undesirable side effects and the emergence of drug resistance may greatly impede their use in clinical progression.[17] An ideal option to circumvent these side effects is to selectively direct the drug accumulation into tumor sites through effective delivery vehicles and to locally activate platinum(II) drugs in a highly controlled manner.[19−23] Up to now, several activatable Pt(IV) complexes by the stimuli of reducing regents[24,25] or light irradiation[26−29] have been developed as attractive prodrugs for controlled cancer therapy.[9] Recently, we have reported an inorganic lanthanide nanopartcle platform to control the localized activation of photoactive Pt(IV) drug within tumor cells.[30,31] Despite its great promise in the in vitro and in vivo studies, the development of a new type of natural delivery platform for photoactivatable Pt(IV)

Received: March 31, 2015
Revised: April 28, 2015
Published: May 4, 2015

DOI: 10.1021/acs.bioconjchem.5b00170
Bioconjugate Chem. 2015, 26, 955−961

prodrug combined with simultaneous evaluation of the corresponding antitumor activities for improved tumor specificity and minimum drug resistance is of clinical importance, and relevant investigations have not been fully exploited so far.

Herein, we introduce a novel and effective drug release system consisting of a specific photoactivatable Pt(IV) prodrug and an apoptosis-responsive probe upon their conjugation with HSA protein carrier. Such light-responsive nanoconjugates can selectively trigger the localized activation of Pt(IV) prodrug, thus greatly improving the anticancer effect of platinum-based therapeutic agents in tumor cells. More importantly, the proposed nanocarriers also provide promising advantages by allowing simultaneous real-time imaging of controlled drug release and evaluation of the corresponding antitumor activities.

RESULTS AND DISCUSSION

Preparation and Characterization of Photoactive Pt(IV)-Probe@HSA Nanocarriers. Figure 1 illustrates the

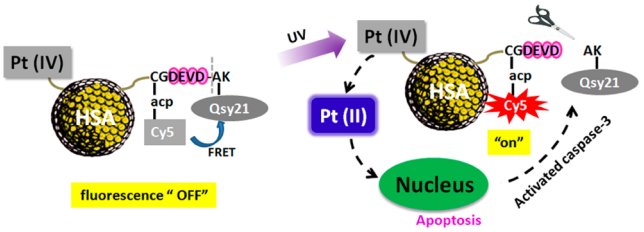

Figure 1. Photoactive Pt(IV) prodrug and peptide probe conjugated HSA nanocarrier for controlled drug activation and real-time imaging of activated apoptosis.

rational design of the light-responsive antitumor Pt(IV) prodrug activation and simultaneous apoptosis imaging based on the smart Pt(IV)-probe@HSA nanocarrier. Typically, HSA nanocarriers were prepared according to the reviously reported desolvation method (Figure S1).[32,33] A photoactivatable Pt(IV) complex *trans,trans,trans*-$[Pt(N_3)_2(OH)(O_2CCH_2CH_2CO_2H)(py)_2]$ (Scheme S1) was chosen as the prodrug to conjugate with amino groups on HSA structures (Scheme 1). One great advantage of such HSA conjugation is to improve the payload capacity due to the abundant distributions of amino groups than other functional groups on the protein surface. Moreover, to achieve real-time apoptosis imaging, an enzyme activatable peptide sequence (e.g., Cy5-acp-CGDEVDAK-Qsy21) flanked with fluorescence resonance energy transfer (FRET) pair

Scheme 1. Schematic Representation for the Synthesis of Pt(IV)-Probe@HSA Nanocarrier[a]

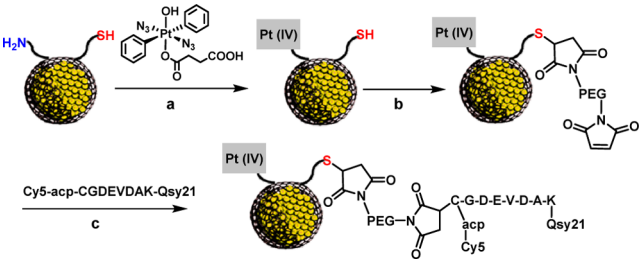

[a]Reagents and conditions: (a) EDC·HCl, DMF, DIPEA, 24 h, rt; (b) Mal-dPEGTM$_6$-Mal, DIPEA, DMF, overnight, rt; (c) Peptide probe Cy5-acp-CGDEVDAK-Qsy21, DIPEA, DMF, 24 h, rt.

containing a near-infrared (NIR) fluorescence donor (Cy5) and a quencher (Qsy21) was conjugated to HSA nanocarrier (Scheme S2). Considering the cysteine group in the HSA protein structure, the thiol-reactive Mal-dPEGTM$_6$-Mal linker was first introduced into HSA nanocarrier to afford maleimide modified HSA nanoconjugates, which could further react with the cysteine in the peptide sequence (e.g., Cy5-acp-CGDEVDAK-Qsy21) through the specific interactions between free thiol and maleimide group (Scheme 1). Such protein based imaging probe is designed for specific response to caspase-3, one of the prerequisite proteolytic enzyme related to cell apoptosis.[34,35] The successful preparation of HSA carrier (Pt(IV)-probe@HSA) was characterized by transmission electron microscope (TEM) and scanning electron microscope (SEM) (Figure 2a,b). The results indicated that Pt(IV)-probe@

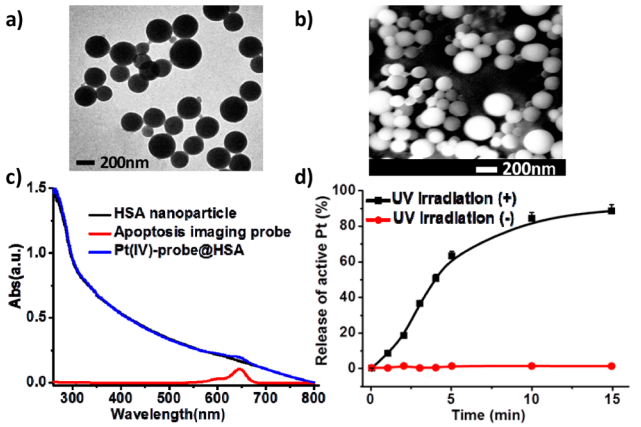

Figure 2. TEM (a) and SEM (b) images of Pt(IV)-probe@HSA nanocarrier; (c) UV−vis spectra of HSA nanoparticle (black), Pt(IV)-probe@HSA (blue) and probe (red); (d) Photoactivation of Pt(IV)-probe@HSA in PBS buffer under increasing irradiation time of UV. The sample without UV treatment is used as control.

HSA particle carriers exhibited narrow size distributions with diameter around 200 nm. Both the ninhydrin assay and inductively coupled plasma spectrometry (ICP) measurements indicated the optimal loading of Pt(IV) prodrug (4.1%) on the surface of HSA nanocarriers, which is comparable to the previously reported platinum drug delivery systems.[23,30] Meanwhile, the conjugation of Cy5 peptide probe to HSA nanocarriers was also confirmed by spectroscopic analysis and the amounts of effective probe on HSA particle surface were determined to be 0.3 nmol/mg (Figure 2c).

Photoactivation of Pt(IV)-Probe@HSA Nanocarriers. Furthermore, we investigated the feasibility of drug release from photoactivatable Pt(IV)-probe@HSA nanocarrier. The controlled release of active Pt(II) from HSA nanocarrier was determined by ICP analysis. Prior to light illumination, there was no obvious drug release from free Pt(IV) prodrug and Pt(IV)-probe@HSA nanocarrier, indicating the stability of Pt(IV) complex and Pt(IV)-probe@HSA under dark conditions. Upon UV light irradiation, increasing Pt(II) release was identified and the release process was dependent on prolonged light exposure. After 10 min of UV exposure, the effective drug release from the Pt(IV)-probe@HSA almost reached the plateau with the value of 80%, which was similar to the drug release from free Pt(IV) prodrug upon the same dosage of light irradiation (Figure 2d and Figure S2). The data clearly showed that the Pt(IV)-probe@HSA could effectively respond to light

DOI: 10.1021/acs.bioconjchem.5b00170
Bioconjugate Chem. 2015, 26, 955−961

illumination, thus allowing the localized control of active Pt release in the tumor cells.

Cytotoxicity Assay upon Light Irradiation. The in vitro anticancer effect was then evaluated in target tumor cells under the control of UV light irradiation. In this study, a well characterized tumor cell line pair, cisplatin susceptible human ovarian carcinoma A2780 cell and cisplatin resistant subline A2780cis cell, was chosen as the target cell line. After 6 h incubation with different concentrations of Pt(IV)-probe@HSA, the cells were exposed to UV light followed by additional 24 h incubation before cell viability assays. As indicated in Figure 3a,b, the photoactivatable cytotoxicity of Pt(IV)-probe@HSA was dependent on the concentrations of Pt and the duration of light irradiation. Under 3 min UV light irradiation, Pt(IV)-probe@HSA (20 μM) showed obvious cytotoxicity toward both A2780 and A2780cis cells with cell viability of 74% and 79%, respectively, and higher concentrations (Pt(IV)-probe@HSA (40 μM)) resulted in more cell death (e.g., 51% and 68% cell viability toward A2780 and A2780cis cells). As control, the cells treated with Pt(IV)-probe@HSA but no UV light irradiation did not show obvious lethality, indicating that UV irradiation of Pt(IV) conjugated HSA nanocarriers was essential for the controlled prodrug activation. Similarly, the treatment of UV light (e.g., 1, 2, 3 min) but without Pt(IV)-probe@HSA incubation did not result in obvious cell lethality to both A2780 and A2780cis cells (Figure S3), suggesting that the potent antitumor activity was mainly from the light triggered Pt(IV) activation. Moreover, illumination of Pt(IV)-probe@HSA incubated cells demonstrated higher antitumor activity when compared to the results observed in free Pt(IV) prodrug or cisplatin treated cells (Figure 3c,d and Figure S4). Clearly, when upon 3 min UV irradiation of Pt(IV)-probe@HSA (40 μM) incubated cells, there was 35% cell lethality observed in drug resistant A2780cis tumor lines, whereas only 20% cell lethality was found in free Pt(IV) prodrug treated cells under same conditions. The results suggested that the combination of photoactivatable Pt(IV) prodrug with HSA nanocarriers indeed offered a promising therapeutic platform to enhance drug efficiency, especially for those cells with potent drug resistant properties.

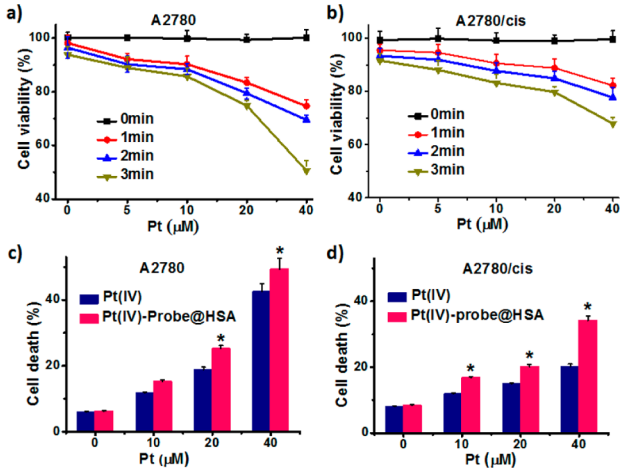

Figure 3. Cytotoxicity assays of Pt(IV)-probe@HSA in A2780 (a) and A2780cis cells (b) with UV light exposure for different time duration (1 min (red ●), 2 min (blue ▲), 3 min (green ▼)), the cells without UV irradiation were used as control (black ■). The cytotoxicity assays of Pt(IV)-probe@HSA (pink) and free Pt(IV) drug (blue) with UV exposure for 3 min in A2780 (c) and A2780cis cells (d). The symbol * means significant difference ($p < 0.05$) between Pt(IV)-probe@HSA and Pt(IV) prodrug.

We further determined the quantitative distribution of effective Pt in cellular nucleus. Basically, after the treatment with free Pt(IV) or Pt(IV)-probe@HSA (20 μM), A2780, or A2780cis cells were exposed to UV for 3 min followed by 24 h incubation. The nucleus DNA was extracted based on standard protocol and the Pt content was determined by ICP analysis (Figure S5). The platination found in free Pt(IV) prodrug treated A2780 and A2780cis cells was 0.18 ± 0.01 and 0.12 ± 0.01 ng Pt/μg DNA, respectively. While enhanced Pt content in cell nucleus were observed to be 0.22 ± 0.01 and 0.18 ± 0.01 ng Pt/μg DNA in A2780 and A2780cis cells after treatment with Pt(IV)-probe@HSA. As contrast, cells treated with Pt(IV)-probe@HSA alone but no UV light irradiation only showed limited Pt distribution in the nucleus. Such quantification of DNA platination is consistent with the trend observed in cell viability tests, further suggesting the advantage of HSA nanocarriers as effective cargo platform for controlled prodrug activation in targeted tumor cells.

Apoptosis Imaging Analysis. In line with the controlled photoactivation of Pt(IV) prodrug, the cytotoxic mechanism was studied by investigating the possibility of Pt(IV)-probe@HSA triggered apoptosis. As proof-of-concept, Pt(IV)-probe@HSA (20 μM) was first incubated with caspase-3/CCP32 (2 unit), one of key executioner protease enzymes in programmed cell death, in HEPES buffer at 37 °C, and the enzymatic hydrolysis was evaluated by measuring the fluorescence changes of Cy5 at 665 nm. After incubation with enzyme for 2 h, there was a 4-fold increase in fluorescence observed (Figure S6). In contrast, enzyme hydrolysis with addition of caspases-3 inhibitor (Ac-DEVD-CHO, 20 μM) revealed very weak fluorescence, indicating that the peptide probe (Cy5-acp-CGDEVDAK-Qsy21) on Pt(IV)-probe@HSA could be used to monitor the activities of caspases-3. We also investigated the capability of Pt(IV)-probe@HSA to real-time evaluate the cellular apoptosis induced by the localized Pt(IV) prodrug light activation in living cells. As shown in Figure 4, upon incubation of Pt(IV)-probe@HSA and 3 min UV irradiation, the remarkable far-red Cy5 fluorescence was detected in both A2780 and A2780cis cells, which implied a disruption of FRET between Cy5 and Qsy21 as a result of the activated caspase-3 caused by the photoactivated cytotoxic Pt(II) components. The occurrence of cell apoptosis was further confirmed by standard annexin V staining that has been widely used in apoptosis identification.[36] As comparison, the similar apoptotic process was also evaluated by incubation of cisplatin antitumor drug with both A2780 and A2780cis cells through the staining of

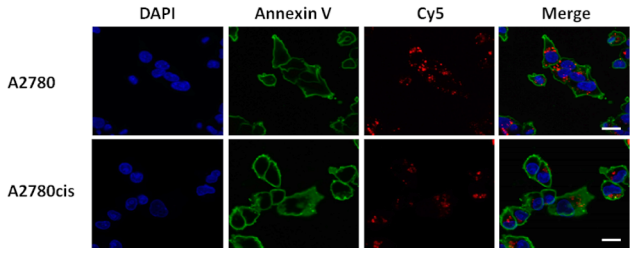

Figure 4. Apoptosis imaging for UV irradiation (3 min) of Pt(IV)-probe@HSA (20 μM) after incubation with A2780 and A2780cis cells. (blue: DAPI; green: Annexin V; red: Cy5). Scale bar = 20 μm.

DOI: 10.1021/acs.bioconjchem.5b00170
Bioconjugate Chem. 2015, 26, 955−961

annexin V (Figure S7). Unsurprisingly, the cisplatin drug showed ineffectiveness toward drug resistant cell lines, which further indicated that our HSA protein delivery platform has great potential for overcoming the issues caused by the drug resistance.

Caspase 3-dependent fluorescence enhancement induced by the photoactivation of antitumor Pt(IV) prodrug on HSA particle surface was also investigated by quantitative flow cytometric (FCM) analysis in the absence and presence of caspase 3 inhibitor (Figure 5). The increasing trend for

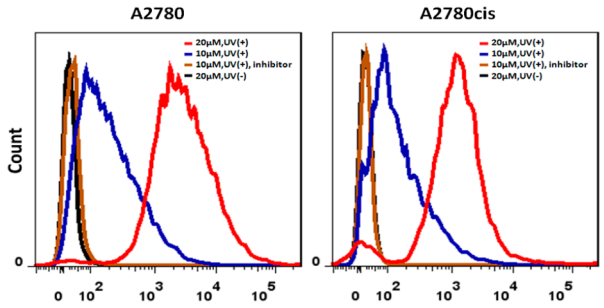

Figure 5. Flow cytometric analysis of A2780 and A2780cis cells treated with different concentrations of Pt(IV)-probe@HSA (10 and 20 μM, respectively) and 3 min irradiation. Cells pretreated with Ac-DEVD-CHO (20 μM) inhibitor and then Pt(IV)-probe@HSA were used as controls.

activated apoptosis fluorescence was in good accordance with the observed cytotoxicity and cell imaging studies, further confirming the signs of apoptosis and the high specificity of Pt(IV)-probe@HSA for activating caspase-3. The results of cell imaging and FCM analysis strongly indicated that Pt(IV)-probe@HSA could serve as a reliable platform for real-time tracking of light controlled drug release in targeted tumor cells.

CONCLUSIONS

In summary, we presented a novel and smart cancer therapeutic nanocarrier with integration of photo-controlled antitumor platinum(IV) prodrug and the apoptosis responsive probe on the surface of HSA protein structure. Upon UV light irradiation, the constructed Pt(IV)-probe@HSA could be locally activated to release the cytotoxic Pt drug and thus efficiently resulted in cell death in both cisplatin-sensitive and -resistant tumor cells. Simultaneously, the turn-on fluorescence in the real-time imaging revealed that activation of Pt(IV)-probe@HSA could induce the cellular apoptosis. Such multifunctional protein based nanocarrier not only could provide a promising strategy to control the localized activation of Pt(IV) prodrug and thus greatly minimize the potential side effects, but more importantly, may also offer us a reliable real-time imaging platform for a drug mechanism study which may thus greatly benefit personalized cancer chemotherapy.

EXPERIMENTAL PROCEDURES

Materials and Methods. Cy5 monoreactive NHS ester was purchased from GE Healthcare Life Sciences. Qsy21 monofunctional NHS ester, recombinant human active caspase-3 and Annexin V, Alexa Fluor 488 Conjugate were purchased from Life Technologies. All amino acids and 2-Chlorotrityl Chloride Resin were purchased from GL Biochem Ltd. (Shanghai). All the other reagents were purchased from Sigma-Aldrich. ^{1}H NMR spectra were recorded on a Bruker AV300 spectrometer (300 MHz). Analytical reverse-phase HPLC analysis was performed on a Shimadzu HPLC system with an Alltima C-18 (250 × 10 mm) column at a flow rate of 3.0 mL/min. Mass spectra (MS) were measured with a Thermo LCQ Deca XP Max for ESI. Transmission electron microscopy images were performed on an FEI EM208S operated at 100 kV. Scanning electron microscopy images were performed on JEOL JSM-7600F operated at 10 kV. The amount of platinum was collected on an Agilent 7700x inductively coupled plasma mass spectrometer (ICP-MS). UV−vis absorption spectra were recorded on a Beckman Coulter DU800 UV−visible spectrophotometer. Fluorescence emission spectra were carried out on a Varian Cary Eclipse fluorescence spectrophotometer. Cell imaging tests were conducted with a Nikon Eclipse TE2000 Confocal Microscope. Flow cytometry was performed on a BD LSR II instrument. Photoirradiation experiments were carried out using a UV lamp (Blak-Ray, B-100AP/R, 100 w/365 nm, intensity: 8.9 mW cm^{-2}).

Synthesis of the Complex *trans,trans,trans*-[Pt-$(N_3)_2(OH)(O_2CCH_2CH_2CO_2H)(py)_2$]. The *trans,trans,trans*-[Pt-$(N_3)_2(OH)_2(py)_2$] complex was synthesized from K_2PtCl_4 according to the reported method.[26] ^{1}H NMR (300 MHz, MEOD): δ = 8.95 (dd, J = 1.8 Hz, 5.4 Hz, 4H), 8.20−8.26 (m, 2H), 7.75−7.82 (m, 4H). ESI-MS: m/z: calcd for $C_{10}H_{12}N_8O_2Pt$ ([M + H]$^+$): 471.07; found: 942.67 ([2M +H]$^+$). Succinic anhydride (60 mg) was added to a solution of *trans,trans,trans*-[Pt$(N_3)_2(OH)_2(py)_2$] (200 mg) in DMF (1 mL) under stirring at 75 °C for 4 h. Then the solution was dried in vacuum. After addition of ether, the precipitate was dried in vacuum to obtain the product. (yield ∼60%). ^{1}H NMR (300 MHz, MEOD): δ = 8.85−8.95 (m, 4H), 8.23 (t, J = 7.5 Hz, 2H), 7.76 (t, J = 6.9 Hz, 4H), 2.58−2.65 (m, 2H), 2.50−2.54. (m, 2H). ESI-MS: m/z: calcd for $C_{14}H_{16}N_8O_5Pt$: 571.09; found 594.07 ([M + Na]$^+$).

Synthesis of Peptide for Apoptosis Imaging. The synthesis of peptide sequence was carried out by Fmoc based solid phase synthesis method with 2-Chlorotrityl Chloride Resin following by the previous report.[30] The Fmoc-6-aminohexanoic acid is abbreviated as Fmoc-acp-OH. The coupling reaction was performed at room temperature using HBTU as a coupling reagent and *N,N*-diisopropylethylamine (DIPEA) as a basic catalyst, respectively, for 2 h. The deprotection of Fmoc group was achieved using a 20% piperidine/DMF solution for 20 min. During the synthesis of acp-Cys(Trt)-Gly-Asp(OtBu)-Glu(OtBu)-Val-Asp(OtBu)-Ala-Lys(Qsy21)-Resin, the Dde protecting group was selectively removed using 2% hydrazine hydrate in DMF for 20 min. Subsequently, the peptide was washed with DMF, followed by addition of Qsy 21 succinimidyl ester (2 equiv) and DIPEA (1.5 equiv), and allowed to stir overnight. The Fmoc group was selectively removed and the resulting peptide acp-Cys(Trt)-Gly-Asp(OtBu)-Glu(OtBu)-Val-Asp(OtBu)-Ala-Lys(Qsy21) was washed with DMF and dichloromethane (DCM), and stirred for 2 h in the presence of 95% trifluoroaceticacid (TFA) to cleave the peptide from the resin and to remove OtBu and Trt protecting group. The peptide was purified by HPLC and characterized by ESI-MS. ESI-MS: m/z: calcd 1612.65 ([M + H]$^+$); found 807.33 ([M+2H]$^{2+}$).

In terms of Cy5-acp-CGDEVDAK-Qsy21 synthesis, the previously achieved acp-CGDEVDAK-Qsy21 was dissolved in DMF (0.5 mL). Cy5 monoreactive NHS ester (1.2 equiv) and DIPEA (6 equiv) were then added to this mixture under stirring for 4 h. The product was purified by HPLC with eluting

DOI: 10.1021/acs.bioconjchem.5b00170
Bioconjugate Chem. 2015, 26, 955−961

system consisting of A (water solution) and B (acetonitrile solution) under a linear gradient, monitored by UV absorbance at 650 nm. The linear gradient stretched over 20 min from $t = 0$ min at 20% solution B to $t = 20$ min at 80% solution B with flow rate of 3.0 mL/min. ESI-MS: m/z: $[M + H]^+$ calcd: 2251.87; found: 1126.82 ($[M+2H]^{2+}$), 751.06 ($[M+3H]^{3+}$).

Synthesis of HSA Nanoparticle. HSA nanoparticles (HSA-NPs) were prepared using an established desolvation procedure.[32] Two hundred milligrams of HSA was suspended in distilled water (2.0 mL), with pH adjusted to 8.0. Self-assembled NPs were generated upon continuous (1 mL/min) addition of desolvating agent ethanol (8.0 mL) under constant stirring at room temperature. After the protein desolvation process, 8% glutaraldehyde aqueous solution (100 μL) was added under constant stirring over a period of 24 h to achieve particle cross-linking. The resulting nanoparticles were purified by three cycles of centrifugation (10 000 rpm, 10 min). The size of HSA-NPs was determined using TEM and SEM. The amino groups on HSA particle surface was analyzed by ninhydrin assay,[37] which were further used for conjugation of photoactivatable Pt(IV) prodrugs.

Synthesis of Photoactive Pt(IV)-Probe@HSA. Scheme 1 illustrated the synthetic process for the photoactive Pt(IV)-probe@HSA. Basically, the carboxyl group of photoactive Pt(IV) complex *trans,trans,trans*-$[Pt(N_3)_2(OH)(O_2CCH_2CH_2CO_2H)(py)_2]$ (100 mg) was activated with 1-ethyl-3-[3-(dimethylamino)propyl]carbodiimide hydrochloride (EDC) (50 mg) in DMF (1 mL) under constant stirring overnight and dark conditions. Then the EDC activated prodrug derivative was mixed with HSA-NPs (200 mg) in the presence of DIPEA (20 μL). The solution was stirred for 24 h under dark conditions at room temperature. The resulting prodrug@HSA conjugates were obtained by centrifugation and washed three times with DMF and diethyl ether, respectively. The as-prepared Pt(IV)@HSA was dissolved in water (1 mL), then added dropwise to a DMF solution (1 mL) containing Mal-dPEGTM$_6$-Mal ester (1 mg). After overnight stirring, the specific interactions between free thiol and maleimide could result in the effective formation of the Mal-dPEGTM$_6$-functionalized HSA nanoparticles, which were collected and washed for three times with DMF. Such Mal-dPEGTM$_6$-Mal conjugated nanoparticle further reacted with apoptosis-sensing peptide probe Cy5-acp-CGDEVDAK-Qsy21 (0.1 mM in 500 μL DMF) for 24 h under stirring in a dark condition at room temperature. After the centrifugation and washing by DMF, the Pt(IV)-probe@HSA conjugates were obtained which were further characterized by spectroscopic and ICP analysis to quantify the efficient loading of photoactivatable Pt(IV) and imaging probes onto HSA nanocarrier surface.

Photoactivation of Pt(IV) Prodrug Complex. As control for UV photoactivation of free Pt(IV) prodrug, the Pt(IV) complex (50 μM in PBS buffer) was irradiated with a UV light source at different time intervals. After irradiation, UV−vis spectra were recorded at room temperature. The ratio of released active Pt (II) component was determined by the changes of absorbance at 294 nm according to the formula (% = $(A_0 - A_i)/A_0 \times 100$, A_0 = the absorbance of the sample without UV irradiation at 294 nm, A_i = the absorbance of the sample with UV irradiation at 294 nm).[28] While in the case of UV photoactivation of Pt(IV)-probe@HSA, Pt(IV)-probe@HSA nanocarrier was first dissolved in PBS buffer (1 mg/mL), the sample was then irradiated with UV light under the same condition with free Pt(IV) complex. After centrifugation to precipitate the nanoparticle, the supernatant of released active Pt component was determined by ICP analysis. Similar experiments without UV light irradiation were also conducted as controls to ensure minimized nonspecific activation of prodrug during the whole process.

Cell Viability Tests by MTT Assay. Generally, the human ovarian carcinoma A2780 cells (ECACC) and its cisplatin resistant A2780cis cells (ECACC) were cultured in RPMI 1640 medium (Gibco) supplemented with 10% fetal bovine serum (FBS, HyClone, USA) at 37 °C and 5% CO_2. In the cell-based phototoxicity tests, cells were irradiated with UV light at different time intervals, followed by 24 h incubation and cell viability tests. For UV light irradiation experiments, the cells were treated with different concentrations of photoactive Pt(IV) prodrug complex or Pt(IV)-probe@HSA for 6 h followed by irradiation with UV light at different time intervals. Subsequently, drug-containing medium was replaced with fresh culture medium and cells were incubated for an additional 24 h before viability tests. The cytotoxicity was evaluated by the standard MTT assays.[37] The absorbance at 570 nm was measured by a Tecan Infinite M200 microplate reader. All experiments were repeated three times to obtain the average values.

Platination of DNA in Cell Nucleus. Cells were seeded in the 6-well plate at a density of 10^6 cells/per well. After 24 h incubation, the cells were treated with either photoactive Pt(IV) prodrug compound (20 μM) or Pt(IV)-probe@HSA (20 μM) for 6 h. The medium was replaced with fresh medium and the cells were irradiated with UV light for 3 min before additional 24 h incubation. Meanwhile, cisplatin (20 μM) was incubated with cells for 24 h. After 24 h incubation, the cells were washed, digested, and collected. The nuclear DNA contents were isolated using Wizard genomic DNA purification kit (Promega, UK) according to the manufacturer's instructions. The DNA samples were further digested in nitric acid and the total Pt content was determined by ICP-MS.

Fluorescence Turn-On of Pt(IV)-Probe@HSA upon Responding to Caspase-3. Caspase-3 (2 unit) were preincubated in reaction buffer (100 mM NaCl, 10% glycerol, 10 mM DTT, 1 mM EDTA, and 50 mM HEPES at pH 7.4) for 30 min at 37 °C before addition of Pt(IV)-probe@HSA (20 μM). Fluorescent spectra were recorded at different time intervals. To confirm the specific enzymatic reaction, the commercially available inhibitor, Ac-DEVD-CHO (20 μM),[38] was preincubated with caspase-3 for 30 min before the addition of Pt(IV)-probe@HSA.

Real-Time Fluorescent Imaging of Tumor Cells Treated with Pt(IV)-Probe@HSA and Cisplatin. Tumor cell lines with 3 × 105 cells per well were cultured in a 35-mm-diameter plastic-bottom μ-dish (ibidi GmbH, Germany) for 24 h prior to treatments with Pt(IV)-probe@HSA conjugates (20 μM) or Cisplatin (20 μM). After 6 h incubation, the medium was changed and the cells were irradiated with UV light for 3 min, followed by further incubation of 24 h. The cells were washed with PBS, and were exposed to fresh medium, and then the apoptosis imaging reagent (Annexin V Alexa Fluor 488 Conjugate) was added. After 15 min incubation, the cells were washed and cellular nuclei staining was performed with DAPI according to the standard protocol provided by the supplier (Life Technologies). The live cell imaging was carried out by using a Nikon Eclipse TE2000 Confocal Microscope with the appropriate instrument filter sets. The excitation filters were set

DOI: 10.1021/acs.bioconjchem.5b00170
Bioconjugate Chem. 2015, 26, 955−961

as 364, 488, and 633 nm for DAPI, Annexin V, and Cy5, respectively.

Flow Cytometric Analysis. Cells were seeded in 6-well plates at a density of 3.0×10^5 cells per well in RPMI 1640 medium and incubated for 24 h. The medium was replaced with Pt(IV)-probe@HSA (10, 20 μM) containing medium and incubated for 6 h, followed by UV irradiation for 3 min and further incubation for 24 h. The cells were harvested with trypsin treatment, washed with PBS for 3 times. The fluorescence intensity was quantified by FACS Calibur flow cytometer (BD Biosciences, USA), and the results were analyzed with *FlowJo 7.6.1* software.

■ ASSOCIATED CONTENT

Ⓢ Supporting Information

The complete chemical synthesis of prodrug complex and the probe Cy5-acp-CGDEVDAK-Qsy21, characterization of HSA particles, activation analysis of Pt(IV) prodrug by UV−vis spectra, phototoxicity of UV irradiation to cells, cell cytotoxicity of cisplatin, platination of DNA, fluorescence spectra of Pt(IV)-probe@HSA after incubation with caspase-3, and fluorescent apoptosis imaging of cisplatin. The Supporting Information is available free of charge on the ACS Publications website at DOI: 10.1021/acs.bioconjchem.5b00170.

■ AUTHOR INFORMATION

Corresponding Authors

*E-mail: Edwinyeow@ntu.edu.sg. Phone: 65-63168759.
*E-mail: bengang@ntu.edu.sg. Phone: 65-63168758.

Author Contributions

‡Xi Li and Jing Mu contributed to this work equally.

Notes

The authors declare no competing financial interest.

■ ACKNOWLEDGMENTS

The authors acknowledge Start-Up Grant (SUG), A*STAR PSF Grant (SERC1121202008), RG64/10, RG11/13, COS research collaboration award in Nanyang Technological University, Singapore.

■ ABBREVIATIONS

HSA, human serum albumin; Pt(IV), prodrug, *trans,trans,trans*-$[Pt(N_3)_2(OH)(O_2CCH_2CH_2CO_2H)(py)_2]$; ICP, inductively coupled plasma spectrometry; TEM, transmission electron microscope; SEM, scanning electron microscope

■ REFERENCES

(1) Peer, D., Karp, J. M., Hong, S., Farokhzad, O. C., Margalit, R., and Langer, R. (2007) Nanocarriers as an emerging platform for cancer therapy. *Nat. Nanotechnol. 2*, 751−760.

(2) Szakács, G., Paterson, J. K., Ludwig, J. A., Booth-Genthe, C., and Gottesman, M. M. (2006) Targeting multidrug resistance in cancer. *Nat. Rev. Drug Discovery 5*, 219−234.

(3) Davis, M. E., and Shin, D. M. (2008) Nanoparticle therapeutics: an emerging treatment modality for cancer. *Nat. Rev. Drug Discovery 7*, 771−782.

(4) Wang, A. Z., Langer, R., and Farokhzad, O. C. (2012) Nanoparticle delivery of cancer drugs. *Annu. Rev. Med. 63*, 185−198.

(5) Ng, K. K., Lovell, J. F., and Zheng, G. (2011) Lipoprotein-inspired nanoparticles for cancer theranostics. *Acc. Chem. Res. 44*, 1105−1113.

(6) Bu, L., Ma, X., Tu, Y., Shen, B., and Cheng, Z. (2013) Optical image-guided cancer therapy. *Curr. Pharm. Biotechnol. 14*, 723−732.

(7) Kim, J., Piao, Y., and Hyeon, T. (2009) Multifunctional nanostructured materials for multimodal imaging, and simultaneous imaging and therapy. *Chem. Soc. Rev. 38*, 372−390.

(8) Chen, Q., Wang, C., Cheng, L., He, W., Cheng, Z., and Liu, Z. (2014) Protein modified upconversion nanoparticles for imaging-guided combined photothermal and photodynamic therapy. *Biomaterials 35*, 2915−2923.

(9) Huang, Y., He, S., Cao, W., Cai, K., and Liang, X.-J. (2012) Biomedical nanomaterials for imaging-guided cancer therapy. *Nanoscale 4*, 6135−6149.

(10) Elzoghby, A. O., Samy, W. M., and Elgindy, N. A. (2012) Protein-based nanocarriers as promising drug and gene delivery systems. *J. Controlled Release 161*, 38−49.

(11) Liu, F., Mu, J., and Xing, B. (2015) Recent advances on the development of pharmacotherapeutic agents on the basis of human serum albumin. *Curr. Pharm. Des. 21*, 1866−1888.

(12) Kratz, F. (2014) A clinical update of using albumin as a drug vehicle-A commentary. *J. Controlled Release 190*, 331−336.

(13) Zhang, S., Kucharski, C., Doschak, M. R., Sebald, W., and Uludağ, H. (2010) Polyethylenimine−PEG coated albumin nanoparticles for BMP-2 delivery. *Biomaterials 31*, 952−963.

(14) Zheng, Y.-R., Suntharalingam, K., Johnstone, T. C., Yoo, H., Lin, W., Brooks, J. G., and Lippard, S. J. (2014) Pt (IV) prodrugs designed to bind non-covalently to human serum albumin for drug delivery. *J. Am. Chem. Soc. 136*, 8790−8798.

(15) Yang, M., Hoppmann, S., Chen, L., and Cheng, Z. (2012) Human serum albumin conjugated biomolecules for cancer molecular imaging. *Curr. Pharm. Des. 18*, 1023−1031.

(16) Galanski, M., Jakupec, M. A., and Keppler, B. K. (2005) Update of the preclinical situation of anticancer platinum complexes: novel design strategies and innovative analytical approaches. *Curr. Med. Chem. 12*, 2075−2094.

(17) Kelland, L. (2007) The resurgence of platinum-based cancer chemotherapy. *Nat. Rev. Cancer 7*, 573−584.

(18) Jung, Y., and Lippard, S. J. (2007) Direct cellular responses to platinum-induced DNA damage. *Chem. Rev. 107*, 1387−1407.

(19) Butler, J. S., and Sadler, P. J. (2013) Targeted delivery of platinum-based anticancer complexes. *Curr. Opin. Chem. Biol. 17*, 175−188.

(20) Wang, X., and Guo, Z. (2013) Targeting and delivery of platinum-based anticancer drugs. *Chem. Soc. Rev. 42*, 202−224.

(21) Min, Y., Mao, C. Q., Chen, S., Ma, G., Wang, J., and Liu, Y. (2012) Combating the drug resistance of cisplatin using a platinum prodrug based delivery system. *Angew. Chem., Int. Ed. 51*, 6742−6747.

(22) Berners-Price, S. J. (2011) Activating platinum anticancer complexes with visible light. *Angew. Chem., Int. Ed. 50*, 804−805.

(23) Pichler, V., Mayr, J., Heffeter, P., Dömötör, O., Enyedy, É. A., Hermann, G., Groza, D., Köllensperger, G., Galanksi, M., and Berger, W. (2013) Maleimide-functionalised platinum (IV) complexes as a synthetic platform for targeted drug delivery. *Chem. Commun. 49*, 2249−2251.

(24) Graf, N., and Lippard, S. J. (2012) Redox activation of metal-based prodrugs as a strategy for drug delivery. *Adv. Drug Delivery Rev. 64*, 993−1004.

(25) Hall, M. D., and Hambley, T. W. (2002) Platinum (IV) antitumour compounds: their bioinorganic chemistry. *Coord. Chem. Rev. 232*, 49−67.

(26) Farrer, N. J., Woods, J. A., Salassa, L., Zhao, Y., Robinson, K. S., Clarkson, G., Mackay, F. S., and Sadler, P. J. (2010) A potent trans-diimine platinum anticancer complex photoactivated by visible light. *Angew. Chem., Int. Ed. 49*, 8905−8908.

(27) Wong, D. Y. Q., Yeo, C. H. F., and Ang, W. H. (2014) Immuno-chemotherapeutic platinum (IV) prodrugs of cisplatin as multimodal anticancer agents. *Angew. Chem., Int. Ed. 126*, 6870−6874.

(28) Mackay, F. S., Woods, J. A., Heringová, P., Kašpárková, J., Pizarro, A. M., Moggach, S. A., Parsons, S., Brabec, V., and Sadler, P. J. (2007) A potent cytotoxic photoactivated platinum complex. *Proc. Natl. Acad. Sci. U.S.A. 104*, 20743−20748.

DOI: 10.1021/acs.bioconjchem.5b00170
Bioconjugate Chem. 2015, 26, 955−961

(29) Zhao, Y., Farrer, N. J., Li, H., Butler, J. S., McQuitty, R. J., Habtemariam, A., Wang, F., and Sadler, P. J. (2013) De novo generation of singlet oxygen and ammine ligands by photoactivation of a platinum anticancer complex. *Angew. Chem., Int. Ed. 125*, 13878−13882.
(30) Min, Y., Li, J., Liu, F., Yeow, E. K., and Xing, B. (2014) Near-infrared light-mediated photoactivation of a platinum antitumor prodrug and simultaneous cellular apoptosis imaging by upconversion-luminescent nanoparticles. *Angew. Chem., Int. Ed. 126*, 1030−1034.
(31) Min, Y., Li, J., Liu, F., Padmanabhan, P., Yeow, E. K., and Xing, B. (2014) Recent advance of biological molecular imaging based on lanthanide-doped upconversion-luminescent nanomaterials. *Nanomaterials 4*, 129−154.
(32) Langer, K., Balthasar, S., Vogel, V., Dinauer, N., Von Briesen, H., and Schubert, D. (2003) Optimization of the preparation process for human serum albumin (HSA) nanoparticles. *Int. J. Pharm. 257*, 169−180.
(33) Ulbrich, K., Michaelis, M., Rothweiler, F., Knobloch, T., Sithisarn, P., Cinatl, J., and Kreuter, J. (2011) Interaction of folate-conjugated human serum albumin (HSA) nanoparticles with tumour cells. *Int. J. Pharm. 406*, 128−134.
(34) Lovell, J. F., Liu, T. W., Chen, J., and Zheng, G. (2010) Activatable photosensitizers for imaging and therapy. *Chem. Rev. 110*, 2839−2857.
(35) Huang, X., Swierczewska, M., Choi, K. Y., Zhu, L., Bhirde, A., Park, J., Kim, K., Xie, J., Niu, G., and Lee, K. C. (2012) Multiplex imaging of an intracellular proteolytic cascade by using a broad-spectrum nanoquencher. *Angew. Chem., Int. Ed. 51*, 1625−1630.
(36) Dumont, E., Reutelingsperger, C., Smits, J., Daemen, M., Doevendans, P., Wellens, H., and Hofstra, L. (2001) Real-time imaging of apoptotic cell-membrane changes at the single-cell level in the beating murine heart. *Nat. Med. 7*, 1352−1355.
(37) Yang, Y., Aw, J., Chen, K., Liu, F., Padmanabhan, P., Hou, Y., Cheng, Z., and Xing, B. (2011) Enzyme-responsive multifunctional magnetic nanoparticles for tumor intracellular drug delivery and imaging. *Chem.—Asian J. 6*, 1381−1389.
(38) McMillan, E. M., and Quadrilatero, J. (2011) Differential apoptosis-related protein expression, mitochondrial properties, proteolytic enzyme activity, and DNA fragmentation between skeletal muscles. *Am. J. Physiol. Regul. Integr. Comp. Physiol. 300*, R531−R543.

DOI: 10.1021/acs.bioconjchem.5b00170
Bioconjugate Chem. 2015, 26, 955−961